fluids

MDPI

Article

Optimizing the Mobile Pump and Its Equipment to Reduce the Risk of Pluvial Flooding

Horas Yosua [1,2,*], Muhammad Syahril Badri Kusuma [3], Joko Nugroho [3], Eka Oktariyanto Nugroho [3] and Deni Septiadi [4]

[1] Doctoral Program of Water Resources Engineering, Faculty of Civil and Environmental Engineering, Institut Teknologi Bandung, Bandung 40132, Indonesia
[2] Water Resources Agency of Jakarta, DKI Jakarta 10150, Indonesia
[3] Water Resources Engineering Research Group, Faculty of Civil and Environmental Engineering, Institut Teknologi Bandung, Bandung 40132, Indonesia; msbadrik2021@gmail.com (M.S.B.K.); joko.nugroho.itb@gmail.com (J.N.); nugrohoeka@itb.ac.id (E.O.N.)
[4] Indonesian School of Meteorology Climatology and Geophysics (STMKG), South Tangerang 15221, Indonesia; deni.septiadi@stmkg.ac.id
* Correspondence: horasyosua85@gmail.com

Abstract: Pluvial flooding in South Jakarta poses significant economic disruptions, requiring efficient mitigation strategies. This study focuses on optimizing mobile pump deployment as a non-structural flood control measure. Despite the use of mobile pumps in flood response, there is limited research on their systematic optimization for pluvial flood mitigation. This study presents a transferable framework for deploying mobile pumps to mitigate pluvial flood risks in urban areas, demonstrated through a case study in South Jakarta, Indonesia. The findings indicate that flood depths of 75 cm have a 20–50% probability of occurrence, and rainfall in South Jakarta follows a distinct hourly distribution, with 56.6% of the rainfall occurring in the first hour and 43.4% in the second. Radar imagery from the BMKG is used here as the main tool for real-time rainfall detection. The optimization framework considers channel capacity, flood frequency, impact severity, accessibility, and operational protocols. Among 29 flood-prone locations analyzed, 8 of them require mobile pump intervention. Seven locations benefit from integration with weather prediction tools and SCADA systems, while three require dedicated operational procedures (SOPs). Simulation results indicate that placing mobile pumps near the upstream section of the flooded area yields the most effective flood reduction. A minimum pump capacity of 0.5 m^3/s is recommended for optimal performance. This study demonstrates that strategic mobile pump deployment, coupled with predictive tools, significantly reduces pluvial flood risks in South Jakarta and offers a transferable framework for other urban areas.

Keywords: depth of flood; mobile pump; pluvial floods; rainfall intensity; South Jakarta; radar

check for updates

Academic Editors: Jaan H. Pu, Prashanth Reddy Hanmaiahgari, Manish Pandey, Bimlesh Kumar and D. Andrew S. Rees

Received: 13 March 2025
Revised: 27 April 2025
Accepted: 29 April 2025
Published: 7 May 2025

Citation: Yosua, H.; Kusuma, M.S.B.; Nugroho, J.; Nugroho, E.O.; Septiadi, D. Optimizing the Mobile Pump and Its Equipment to Reduce the Risk of Pluvial Flooding. *Fluids* **2025**, *10*, 119. https://doi.org/10.3390/fluids10050119

Copyright: © 2025 by the authors. Licensee MDPI, Basel, Switzerland. This article is an open access article distributed under the terms and conditions of the Creative Commons Attribution (CC BY) license (https://creativecommons.org/licenses/by/4.0/).

1. Introduction

Flooding has been a persistent issue in Jakarta, with records dating back to 1963. Despite continuous improvements in flood control infrastructure, the number of flood-prone areas has continued to grow. Several factors contribute to this, including increased rainfall intensity, changes in land use, and the limited capacity of existing drainage systems.

Jakarta experiences two types of flooding: fluvial and pluvial floods. Historically, floods in Jakarta were primarily fluvial, occurring along riverbanks. However, in recent years, there has been a shift towards pluvial flooding, where intense rainfall overwhelms

urban drainage systems, causing waterlogging in built-up areas far from rivers. Pluvial floods [1–4] present a significant challenge due to their sudden onset and short duration, making conventional flood mitigation strategies less effective.

Flood mitigation in Jakarta has primarily relied on structural approaches such as river normalization, diversion channels (sodetan), and polder systems [5–9]. However, these approaches are becoming increasingly challenging due to rapid urbanization and limited land availability for new drainage infrastructure. Expanding drainage channels to accommodate a 5-year return period flood, for example, would require much larger dimensions (100 cm $\times$ 100 cm) than what is feasible in Jakarta's densely built environment.

As an alternative, non-structural flood control measures are gaining attention. One such approach is the use of mobile pumps to actively manage floodwaters by relocating excess water from flood-prone areas to locations with available drainage capacity. Papers discussing the mobile pump framework have been published by Cheng et al. [10] and Li et al. [11]. Kapsiz [12] presented the energy efficiency of a diesel engine. Other papers [13–17] discuss stationary pumps. Despite these advances, the literature lacks a systematic methodology for optimizing mobile pump placement and operation in urban pluvial flood scenarios. Current studies treat hydrological models, hydraulic simulations, and meteorological data as separate entities rather than components of an integrated framework. This fragmented approach limits the practical applicability of mobile pumps in real-time flood management.

With pluvial floods increasing in frequency due to climate change and urbanization, there is an urgent need for innovative, adaptable solutions. This study fills the identified gap by proposing an optimization framework that combines real-time data and mobile pump deployment strategies. Such an approach is critical for enhancing urban flood resilience, particularly in resource-constrained environments where traditional infrastructure is impractical. The novelty of this study lies in its systematic approach to optimizing mobile pump deployment for pluvial flood mitigation, achieved through the integration of hydrological, hydraulic, and real-time meteorological data.

This is the first study to combine BMKG radar data with HEC-RAS simulations and operational protocols (e.g., SCADA) to enhance urban flood resilience. As illustrated in Figure 1, mobile pumps play a critical role in non-structural flood control by actively managing floodwaters. Our study aims to optimize their deployment through data-driven strategies. This study evaluates flood risks by analyzing key parameters such as rainfall intensity, flood depth, and flood duration, ensuring a data-driven understanding of flood-prone areas. To enhance predictive capabilities, BMKG (Indonesian Meteorological, Climatological, and Geophysical Agency) radar imagery is utilized for real-time rainfall monitoring and lead-time forecasting, allowing for proactive flood management.

Furthermore, this research develops an optimized pump deployment strategy that considers site-specific constraints, accessibility, and operational protocols, ensuring that mobile pumps are deployed efficiently in locations where they can provide the greatest impact.

This study aims to develop an optimization framework for mobile pump deployment in South Jakarta, ensuring more effective flood mitigation strategies. To achieve this, our research first analyzes the relationship between rainfall intensity, flood depth, and drainage capacity in flood-prone areas, providing insights into how these factors interact in urban flooding scenarios. Following this, this study assesses the effectiveness of mobile pumps in reducing flood depth and duration, determining their impact on flood mitigation efforts.



Figure 1. Mobile pumps in operation.

A key aspect of this research is the identification of priority locations for mobile pump placement based on flood risk criteria, ensuring that pumps are deployed where they are needed most. Additionally, this study evaluates integration strategies that incorporate weather prediction tools, such as BMKG radar, and operational control systems, including SCADA, to improve real-time flood management. Finally, to validate the proposed optimization framework, we conducted simulations using hydraulic modeling tools, such as HEC-RAS, to assess the performance and effectiveness of the recommended pump deployment strategies.

By addressing these objectives, this study provides a structured methodology for optimizing mobile pump use in urban flood management, offering insights that can be applied to other cities facing similar challenges.

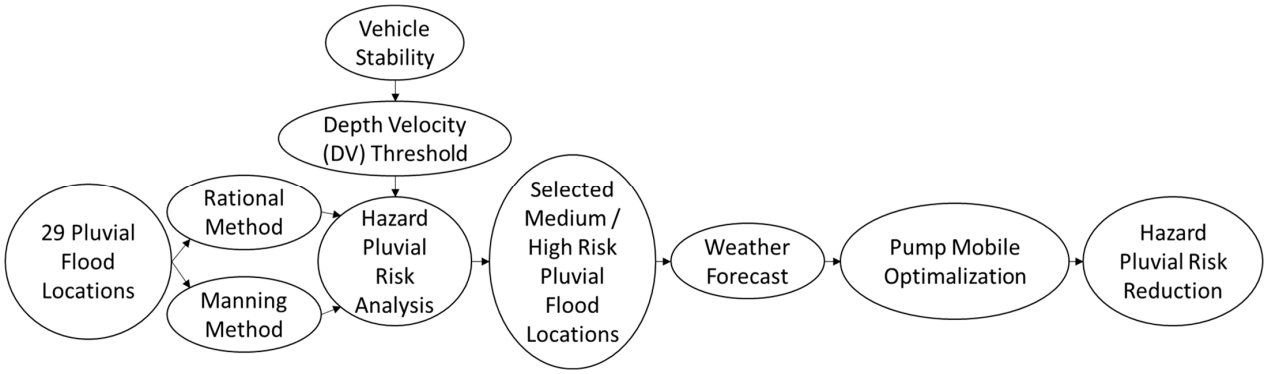
2. Methodology

2.1. Mobile Pump Deployment Optimization

This study follows a structured framework, as illustrated in Figure 2, to analyze flood characteristics and evaluate the effectiveness of mobile pump deployment in mitigating pluvial flooding. The methodology begins with an assessment of drainage system limitations, comparing planned flood discharge with the existing channel capacity. The planned flood discharge is determined based on a rainfall intensity of 15 mm/h, using a rational method.

A rainfall–runoff model was applied to estimate the flood discharge under different storm conditions. The rational method uses a simple $Q = CIA$ formula, where Q is the runoff discharge (m^3/s), C is the runoff coefficient, I is the rainfall intensity (mm/h), and A is the catchment area (km^2). Meanwhile, to assess the drainage capacity, Manning's equation $Q = \frac{1}{n} A R^{\frac{2}{3}} \sqrt{S}$ was applied, where n is Manning's roughness coefficient, A is the cross-sectional area, R is the hydraulic radius, and S is the channel slope. These calculations were used to compare planned flood discharges with the capacity of the existing drainage system under different return periods (5-year, 10-year, etc.). The equation assumes uniform flow, where the water's depth and velocity remain constant along the channel, and steady-state conditions, where inflow equals outflow. These assumptions simplify the complex dynamics of urban runoff but are considered to be suitable for initial assessments of channel capacity in small urban catchments (≤ 1 km^2), as in South Jakarta. We later solve

the limitations of Manning's equation in urban settings that assume subcritical flow and do not account for transient effects like backwater or non-uniform flow caused by urban obstacles (e.g., debris, man-made structures), by incorporating it with the rational method.



Two conditions for hydrological and hydraulic analysis.

Condition				Remarks
1	Insufficient channel capacity	a	Flood frequency	Zero flooding does not require a mobile pump.
		b	Impact of flood depth and flood duration	Floods below a flood depth of 75 cm or a flood duration of 30 min does not require a mobile pump.
		c	Inlet, storage, and outlet condition	A pump selection requires head, capacity, and efficiency for design. This depends on the inlet, pump location (storage), and outlet.
		d	Mobile pump entry access, and number of mobile pumps	There are several locations where it is not possible to enter mobile pumps, and there are limited numbers of mobile pumps in South Jakarta.
		e	Mobile pump equipment requirements	The presence of a mobile pump needs to be optimized with radar if flooding still occurs.
2	Sufficient channel capacity	a	Flood frequency	Zero flooding does not require a mobile pump.
		b	Impact of flood depth and flood duration	Floods below a flood depth of 75 cm or a flood duration of 30 min do not require a mobile pump.
		c	Correlation of D (inundation height) and R (rainfall intensity)	If D and R are not linear, then the possible cause of flooding is due to rubbish, wastewater discharge, sedimentation, or other causes.
		d	Mobile pump entry access, and number of mobile pumps	There are several locations where it is not possible to enter mobile pumps, and there are limited numbers of mobile pumps in South Jakarta.
		e	Mobile pump equipment requirements	The presence of a mobile pump needs to be optimized with radar if flooding still occurs.
		f	Mobile pump SOP	If there is a mobile pump, the SOP for the mobile pump that needs to be created is the use of radar, monitoring the inlet channel, activating the mobile pump, and the condition of the mobile pump.

Figure 2. Mobile pump optimization framework.

In our case, HEC-RAS was used to simulate open-channel flow, leveraging Manning's equation to compute water surface profiles based on channel geometry and cali-

brated roughness coefficients (n = 0.013–0.015 for concrete-lined channels in South Jakarta). While Manning's equation assumes subcritical, uniform flow, HEC-RAS accounts for complex urban conditions—such as backwater effects and non-uniform flow due to debris or structures—by solving the Saint-Venant equations. The model results were validated against 2022–2023 flood events. Separately, the peak runoff discharge was estimated using the rational method, adjusted for land cover (e.g., residential, roads) via the C-equivalent approach, to reflect South Jakarta's heterogeneous landscape. This Q served as an input to HEC-RAS, bridging the hydrological and hydraulic analyses despite the rational method's simplifying assumptions of uniform rainfall and steady-state runoff.

These fluid dynamics principles underpinned our hydraulic analysis, enabling us to compare planned flood discharges with channel capacities and identify locations requiring mobile pump intervention. The integration of these methods with real-time weather data (BMKG radar) and hydraulic simulations (HEC-RAS) enhanced the precision of our flood mitigation strategy.

To quantify flood risks, two primary risk thresholds were defined: First, a flood depth threshold defined any location experiencing a flood depth over 75 cm as high risk. Papers [18,19] indicate that a flood height range of 75–80 cm is considered to high-risk and can cause severe damage to infrastructure. More specifically, the 75 cm threshold comes from a diecast model test performed by one of the authors at Institut Teknologi Bandung in 2023 (another manuscript in progress). Second, a flood duration threshold defined any areas where flooding lasts more than 30 min as significantly disruptive [6]. A risk ranking was then developed by analyzing flood frequency from the 2022–2023 records. This provided a basis for prioritizing mobile pump deployment.

To further characterize pluvial flooding, this study examined the relationship between rainfall intensity (R), flood depth (D), and flood area (A), while also considering the presence or absence of mobile pumps at specific flood locations. This comparison highlights the potential influence of mobile pumps in reducing flood severity. To do that, a quadrant-based form was developed to establish correlations among those four events from a single location. Each event within the quadrant was derived from video recordings of four flood events, which were then put into a quadrant-based form, offering an empirical basis for flood behavior analysis. The optimization then followed two situations, as illustrated in Figure 2. The relationships identified in this quadrant were further examined, where the data were plotted against the flood height risk threshold of 75 cm. The summarized correlation results produced a refined understanding of flood risk patterns. Later, from this correlation, we found that weather has a significant influence on rainfall intensity, which we also discuss in this paper with respect to weather data collection. By structuring this study in this manner, our research framework provides a systematic foundation for subsequent methodological steps, including data collection, flood risk assessment, and mobile pump optimization, as discussed in the following sections.

The mobile pump placement strategy was developed using the following criteria: First, drainage capacity deficit was used to define locations where flood discharges exceed the channel capacity, which were identified as priority sites. Second, flood risk assessment was used to determine priority sites based on flood depth ($\geq$75 cm) and duration ($\geq$30 min). Third, the accessibility constraints were used to classify locations with road widths less than three meters, which were excluded due to pump mobility limitations. Fourth, the pump capacity requirements were used to define selection according to head losses, inlet/outlet conditions, and estimated flood discharge. The fifth criterion was the integration with real-time weather prediction. This is where BMKG radar and SCADA were integrated in our analysis for decision-making, i.e., additional SOPs.

Stationary pumps serve the same function as mobile pumps [4,18]; however, the two differ significantly in storage volume. When deployed in flood-prone areas, mobile pumps have minimal storage capacity, typically relying on local microchannels. This limitation is due to the scarcity of available land in urban environments.

To determine the required flood volume storage that must be discharged, a cumulative flood volume curve was analyzed using the Cumulative Distribution Function (CDF). In this process, the smallest possible storage volume was identified while maximizing the mobile pump capacity. However, selecting the highest mobile pump capacity must still account for head requirements, efficiency, and inlet and outlet conditions.

The selection of a mobile pump requires evaluating both the system characteristic curve and the pump performance curve. The operating point of the pump was determined at the intersection of these two curves, meaning that the head value and required capacity dictate the appropriate mobile pump selection. The selection of the head and capacity itself was then calculated based on energy conservation schemes.

Figure 3 illustrates a mobile pump with inlet and outlet placement in an urban drainage scenario. In this case, the water levels at the inlet and outlet are equal, meaning that (HB − HA) = 0. This condition is common in urban drainage systems, particularly in Jakarta, due to the low land slope. However, in some cases where the inlet and outlet are positioned within the same catchment area and hydrological system, the outlet water level (HB) may be higher than the inlet water level (HA). When this occurs, the pump head (H_{pump}) must compensate for the difference. This condition often leads to backwater effects, where water flows from the outlet back into the inlet, potentially disrupting the drainage efficiency.

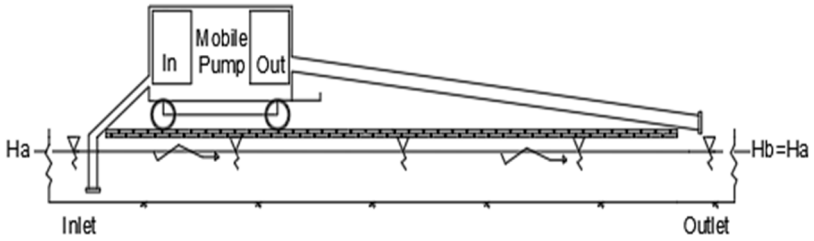


Figure 3. An illustration of a mobile pump, with inlet and outlet.

If backwater effects occur, the outlet location should be reconsidered to prevent inefficiencies. In some cases, the outlet may be connected to a different hydrological system than the inlet, but in such situations, head losses must be carefully assessed. Additionally, the placement of the pump's inlet is critical. Aside from ensuring that the inlet water level is equal to or higher than the outlet water level (HA − HB $\geq$ 0), the inlet location must be free of solid particles, garbage, and sedimentation. Accumulated debris can impair the pump's functionality, preventing it from efficiently draining floodwater.

Thus, the outlet and inlet placement must be carefully considered in relation to the required pump head, hydrological system compatibility, and obstruction-free conditions to ensure efficient mobile pump performance.

In drainage channels with limited capacity, a mobile pump with a capacity adjusted to compensate for hydraulic deficits is necessary. Additionally, accessibility considerations must be taken into account when deploying mobile pumps. For instance, mobile pumps cannot be transported to locations where the road width is less than 3 m. If an analysis determines that the flood depth or duration exceeds the acceptable limits, additional equipment—such as weather prediction tools—is required. These measures are implemented in areas where the existing drainage infrastructure cannot accommodate the planned flood discharge.

In drainage channels with sufficient capacity, an initial analysis is necessary to examine the correlation between rainfall intensity (R) and flood depth (D). This analysis helps determine whether flooding is caused by drainage limitations or other factors. If a mobile pump is already present in the area, a Standard Operating Procedure (SOP) must be established for its operation.

Furthermore, additional mobile pumps may be required to maintain the flood depth below 75 cm and ensure that the flood duration does not exceed 30 min in flood-prone locations. Similar to low-capacity channels, supplementary tools such as weather prediction systems should be integrated if the flood conditions exceed the established depth and duration thresholds.

To validate the optimization approach, mobile pump configurations were tested using hydraulic modeling tools. Simulations using HEC-RAS were conducted under different deployment scenarios to assess their effectiveness. For the modeling approach, hydraulic simulations were performed using calibrated flood models with input parameters including historical flood hydrographs, mobile pump performance curves, and various deployment configurations (upstream, midstream, downstream), while the performance metrics ensured the effectiveness of each deployment strategy. This was measured based on the reduction in flood peak depth and decrease in flood duration. These results were analyzed to determine the optimal mobile pump placement strategy for pluvial flood mitigation.

2.2. Weather Data Collection

This study takes an area focus on South Jakarta, a region frequently affected by pluvial flooding due to its limited drainage capacity and increasing rainfall intensities. To support the analysis, various weather prediction and flood assessment methods were considered, each offering distinct advantages and limitations. The weather data here are strongly related to the definition of the rainfall intensity parameter.

Various weather prediction and flood assessment methods offer different trade-offs in terms of accuracy and lead time. As illustrated in Figure 4, ground-based sensors such as AWLRs provide the highest accuracy but lack real-time availability, while Numerical Weather Prediction (NWP) offers longer lead times but is constrained by computational complexity. Given these trade-offs, this study selected BMKG radar reflectivity data and geospatial satellite imagery as the primary data sources, as they provide a balance between accuracy, real-time applicability, and spatial coverage, making them well suited for flood risk assessment and mobile pump optimization. The selected method provides real-time rainfall monitoring, enabling immediate flood response. Also, taking references from [19–23], we justified that our data, sourced from geospatial and satellite data, offer insights into land use, elevation models, and hydrological basin characteristics, which can help refine flood risk assessments.

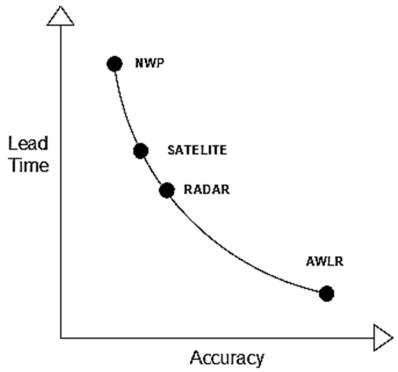


Figure 4. Methods for weather prediction compared in terms of accuracy vs. real-time availability.

The BMKG radar system was chosen due to its ability to detect rainfall intensity with high spatial and temporal resolution, making it a valuable tool for early flood warning and mobile pump deployment decisions. Meanwhile, geospatial and satellite data were used to analyze flood-prone areas, assess drainage system capacity, and evaluate land-use impacts on flood vulnerability. To further enhance flood response strategies, this study also integrated weather prediction tools with the Supervisory Control and Data Acquisition (SCADA) system. The SCADA system, which incorporates sensors, Programmable Logic Controllers (PLCs), and a Human–Machine Interface (HMI), enables real-time water management and facilitates the automated operation of mobile pumps [24–26]. A further analysis, incorporating recursive feature elimination as a preprocessing step to optimize the logistic regression model, was carried out to define the correlation relevance from weather data (radar and satellite). The collected data were analyzed to assess rainfall–runoff relationships, flood risks, and the effectiveness of mobile pumps in mitigating pluvial flooding.

3. Results and Discussion

3.1. Assessing Channel Capacity over Flood Occurrences

Using the rational method and Manning's drainage capacity formula, we obtained the results of the planned flood discharge calculations, assuming a rain intensity of 15 mm/h, and the results of the hydraulic analysis calculations are shown in Table 1.

The rational method that was used to estimate the flood discharges was based on a rainfall intensity of 15 mm/h. The choice of intensity of 15 mm/h in the flood discharge calculation is the smallest intensity capable of causing flooding at the Seskoal Ciledug location, with a planned flood of 0.84 m^3/s. The results, summarized in Table 1, indicate that several drainage channels cannot accommodate the planned discharge, leading to surface water accumulation and localized flooding.

Flood forecasting in small drainage basins presents a significant challenge due to uncertainties in hydrological input variables, in terms of both spatial and temporal resolution. Studies on mobile crowdsensing of water levels have demonstrated that limited data availability complicates flood prediction efforts in such basins. In this study, a rainfall intensity of 15 mm/h was selected as the threshold for flood discharge calculations, as this intensity was observed to cause flooding at the Seskoal Ciledug location, producing a planned flood discharge of 0.84 m^3/s. Based on hydrological analysis using the rational method, the minimum planned flood discharge was found to be 0.50 m^3/s, the maximum 4.33 m^3/s, and the average 1.57 m^3/s for the study area.

Through hydraulic analysis calculations using Manning's empirical calculations, we found that the channel capacities in all 29 locations prone to flooding in South Jakarta locations ranged from a minimum of 0.16 m^3/s to a maximum of 13.06 m^3/s, with the average capacity of channels prone to flooding in South Jakarta being 1.94 m^3/s. If we compare the average value of the planned flood discharge intensity of 15 mm/h (1.57 m^3/s) with the average value of the channel capacity above (1.94 m^3/s), it can be concluded that the average channel in a location vulnerable to pluvial flooding in South Jakarta is able to accommodate the planned discharge with an intensity of 15 mm/h.

Taking an example from the Gandaria City location, the channel capacity is limited to 2.41 m^3/s, while the peak planned discharge is 2.65 m^3/s, resulting in an excess of 0.24 m^3/s, which could lead to localized flooding at peak flow conditions. To mitigate this, a mobile pump with a minimum capacity of 0.25 m^3/s is required to reduce the flood depth and duration. The optimization of mobile pumps' performance can be achieved through weather prediction tools, SCADA integration, storage capacity management, and Standard Operating Procedures (SOPs). However, hydraulic calculations suggest that additional drainage capacity is necessary at this location, presenting a land availability constraint.

Given these limitations, mobile pumps remain the most viable solution for addressing pluvial flooding in South Jakarta.

Table 1. Calculation results of hydrological analysis, hydraulic analysis, and flood frequency in 2022 and 2023.

Nu	Location	Qr 5 Years (m^3/d)	Qr 15 mm/h (m^3/d)	Qr 50 mm/h (m^3/d)	Qc (m^3/d)	Qc/Qr 15 mm/h	Qc/Qr Rank	# Flood Occurrence Frequency in 2022	# Flood Occurrence Frequency in 2023
26	Batu Belah	3.83	3.13	10.43	0.09	0.03	1	5	0
25	Cupang	4.36	0.58	1.93	0.04	0.06	2	4	2
24	Balai Rakyat	9.15	3.16	10.54	0.19	0.06	3	3	2
29	Tebet Barat Dalam	6.29	2.05	6.83	0.34	0.17	4	4	4
15	RW07 Pondok Labu	3.00	0.77	2.56	0.16	0.21	5	0	0
8	Dinas Pendidikan	8.66	2.84	9.46	0.62	0.22	6	3	5
28	Double Track	7.91	3.38	11.25	1.02	0.30	7	0	0
17	Masjid Al Makmur	2.47	0.50	1.66	0.16	0.32	8	0	0
19	Gedung Film	3.13	1.07	3.55	0.34	0.32	9	0	0
4	Terogong Raya	5.21	0.86	2.85	0.30	0.36	10	1	0
18	FO MT Haryono	3.55	0.87	2.88	0.34	0.39	11	0	1
12	Jenderal Sudirman	11.51	1.99	6.62	0.78	0.39	12	0	0
6	Balai Kartini	8.66	2.84	9.46	1.24	0.44	13	0	1
9	Permata Suite	5.16	3.12	10.40	1.70	0.55	14	2	7
23	Komplek Depsos	2.99	0.28	0.93	0.16	0.56	15	0	0
21	JI. HR Rasuna Said	1.55	0.50	1.66	0.34	0.68	16	1	0
5	Karang Tengah	3.76	2.13	7.11	1.48	0.69	17	4	0
1	Gandaria City	4.44	2.65	8.82	2.41	0.91	18	9	8
11	Kapten Tendean	3.78	0.67	2.25	0.75	1.11	19	1	0
22	Semanggi Bawah	2.43	1.02	3.40	1.45	1.42	20	0	0
16	ITC Fatmawati	6.07	1.31	4.36	2.33	1.78	21	6	3
20	Atmajaya	2.43	1.02	3.40	2.36	2.31	22	0	0
13	Terowongan Jend. Sudirman	2.43	1.02	3.40	2.59	2.53	23	0	0
10	Kemang Raya	5.16	0.76	2.55	2.33	3.05	24	7	
27	Asem Baris Raya	5.47	1.08	3.61	3.68	3.40	25	2	6
14	Dharmawangsa Taman Gajah	4.27	3.74	12.46	13.06	3.49	26	4	1
7	Kemnaker RI	3.50	0.73	2.45	3.43	4.67	27	3	1
2	Seskoal Ciledug	4.44	0.84	2.79	4.82	5.76	28	16	11
3	Mabes Polri	5.42	0.67	2.24	7.75	11.53	29	2	0

Notes: Qr = planned flood discharge; Qc = channel capacity discharge.

3.2. Correlation of Parameters

Figure 5 presents data on flood events, detailing daily rainfall intensity, flood depth, and cumulative flood volume in locations where mobile pumps were deployed. The thicker blue areas in the figure represent untreated flood volumes, indicating instances where the drainage infrastructure was insufficient. The comparison between rainfall intensity, flood depth, and flood volume was conducted at Seskoal Ciledug, Gandaria City, and Dharmawangsa Taman Gajah.

Several key observations can be drawn from this situation. First, rainfall distribution is not uniform across South Jakarta. This is evident from the data recorded at the Pondok Labu pump station, where a high rainfall intensity of 69.5 mm/day did not result in flooding, while at Dharmawangsa Taman Gajah, a lower intensity of 23.5 mm/day caused significant flooding. Both events occurred on the same date, indicating that flooding is not solely determined by rainfall intensity but is also influenced by sedimentation, debris accumulation, and drainage efficiency. Second, mobile pumps effectively reduce flood heights, but their timing and location configuration significantly impact their performance. For example, at the Gandaria City location, a 24 mm/day rainfall event resulted in a greater flood volume compared to a 47 mm/day event, demonstrating the importance of proper mobile pump activation and placement. These findings highlight the need for a Standard Operating Procedure (SOP) to optimize mobile pump deployment in flood-prone areas.

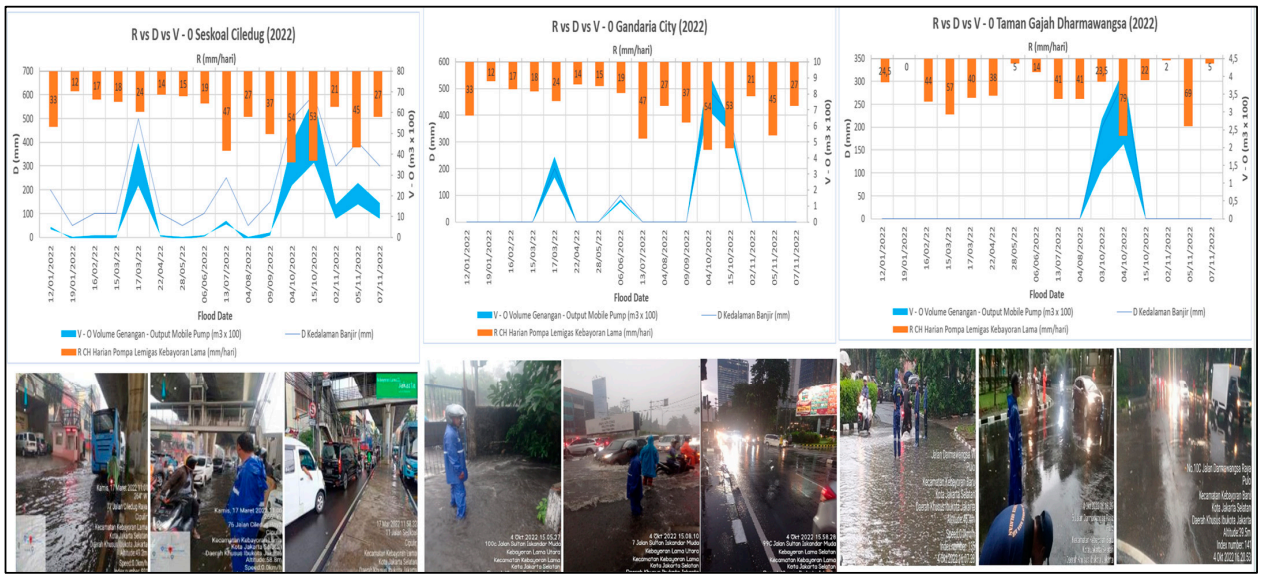


Figure 5. Rainfall intensity, flood depth, and flood volume.

The relationship between flood depth (D) and flood area (A) is critical in assessing flood hazards. To analyze this, we used a quadrant-based form analysis, as illustrated in Figure 6. We set four flood events at the same location (Seskoal Ciledug). The events were selected based on the availability of video data and rainfall records from the Lemigas pump station. The selected flood events occurred on 1 December 2022, 4 January 2023, 26 April 2023, and 24 November 2023. Video recordings were used to conduct field surveys, and Google Earth mapping was utilized to plot the floods' extent by identifying the coordinates of the inundated areas.

The flood characteristics at this site reveal that pluvial flood behavior varies significantly across locations, influenced by site conditions and non-uniform rainfall patterns. A quadrant analysis was conducted to examine the correlation between flood area (A), flood depth (D), and rainfall intensity (R). The quadrant analysis showed that the strongest linear correlation exists between flood area (A) and rainfall intensity (R).

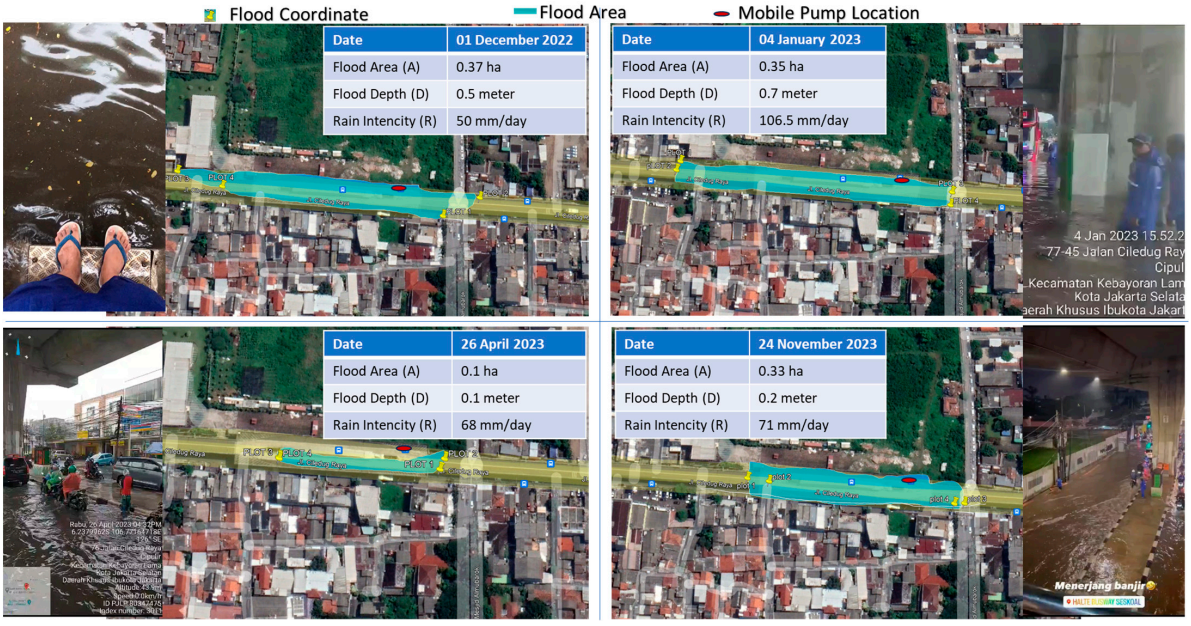


Figure 6. A quadrant-based form analysis to obtain correlations among the A, D, and R variables at different time.

However, when broken down into individual parameter relationships following the quadrant analysis, the closest linear correlation was observed between flood area (A) and flood depth (D), described by the equation $y = 1.5679x - 0.0758$. The relationships between these parameters were analyzed using linear regression models, as depicted in Figure 7 and Table 2. The quadrant-based analysis at Seskoal Ciledug, based on four flood events, provided initial insights into the relationships between A, D, and R. Table 2 presents the outcomes, with limited statistical robustness (e.g., $R^2 = 0.5152$ for A vs. D).

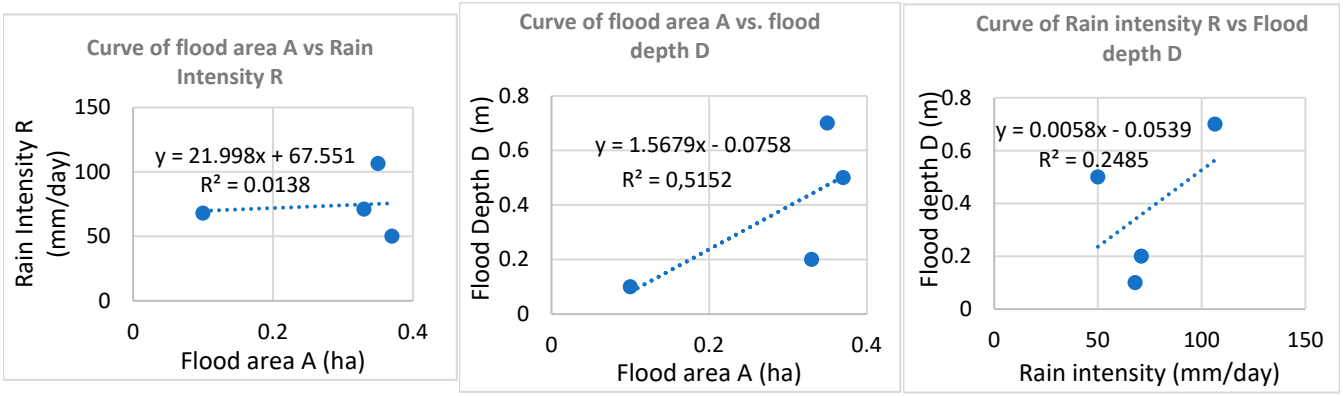


Figure 7. Correlation plots for each parameter.

Table 2. Correlations among parameters A, D, and R.

Nu	Correlation	Coefficient of Determination (R^2)	Correlation Coefficient (R)	Correlation Level
1	A—R	0.0138	0.1174	Very weak
2	R—D	0.2485	0.4985	Moderate
3	A—D	0.5152	0.7178	Strong

The observed deviations from this correlation can be attributed to site-specific factors, such as sedimentation and drainage efficiency, and non-uniform rainfall patterns across South Jakarta. For instance, a rainfall intensity of 23.5 mm/day caused significant flooding at Dharmawangsa Taman Gajah, while 69.5 mm/day at Pondok Labu did not, highlighting spatial rainfall variability and measurement inaccuracies in flood depth estimations, as the depth assessments relied on manual measurements rather than standardized sensors. Taking another look at Table 1, it is noticeable that Seskoal Ciledug, the location from which the quadrant analysis data were taken, has sufficient channel capacity. Considering the framework in Figure 2 once more, for these reasons, the non-uniform rainfall (R) is strongly suspected to have a more significant impact on flood depth (D).

The use of quadrant-based analysis, as shown in Figure 6, along with the individual parameter correlations in Figure 7, although statistically limited, has been acknowledged in some papers. The authors of [27] suggested that a small sample size can still yield meaningful insights. For that reason, they suggested the use of the higher-order linear moment (LH-moment) method to leverage the limitations. The authors of [28] discussed model selection for small samples and emphasized objective techniques. In our case, this variability necessitated the integration of BMKG radar data, which provide real-time, high-resolution rainfall monitoring to overcome non-uniform rainfall patterns, and to improve flood prediction and mobile pump deployment. We opted for BMKG radar-based weather prediction tools to leverage the rainfall data, due to their ability to provide real-time, location-specific rainfall data that are critical for mobile pump deployment in South Jakarta's urban flooding context. While advanced statistical methods could offer deeper

insights, they require extensive datasets and computational resources that were unavailable in this study, making them less feasible for operational, time-sensitive flood management.

3.3. Weather Prediction and Its Role in Mobile Pump Deployment

Pluvial floods occur rapidly, making it essential to analyze hourly rainfall distribution, particularly in South Jakarta (the study area). Several hourly rainfall distribution models have been developed in Indonesia, including Tadasi Tanimoto's 1969 [29] model for Java Island, which adopts an 8 h rainfall distribution, Wanny's model for West Java, which incorporates 3 h and 8 h distributions, and the Directorate General of Water Resources' PSA 50 model, which applies a 6 h distribution [29,30].

This study evaluated hourly rainfall distribution patterns in Jakarta, specifically analyzing rainfall events that triggered flooding in South Jakarta. The Automatic Rainfall Record (ARR) data collected from the Gunung Sub-District station between 2022 and 2024 reveal that rainfall was highly concentrated in the first two hours, with 56.6% occurring in the first hour and 43.4% in the second hour (Figure 8). Given this rainfall pattern, rapid mobile pump deployment within the lead time is crucial to mitigating flood risks in South Jakarta.

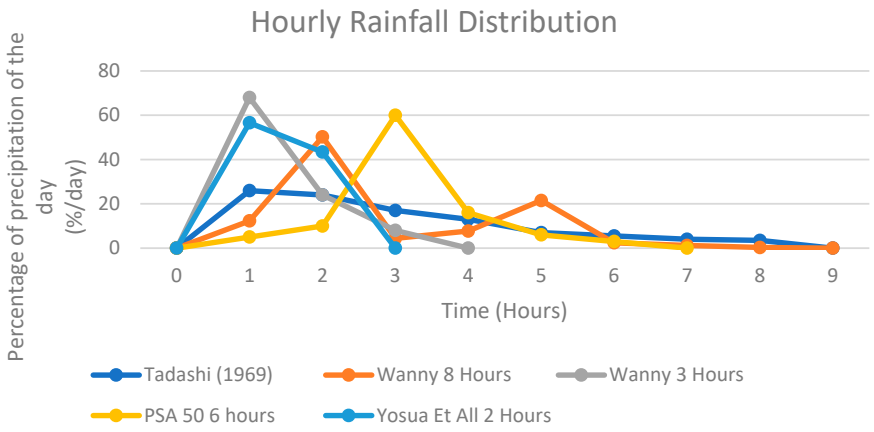
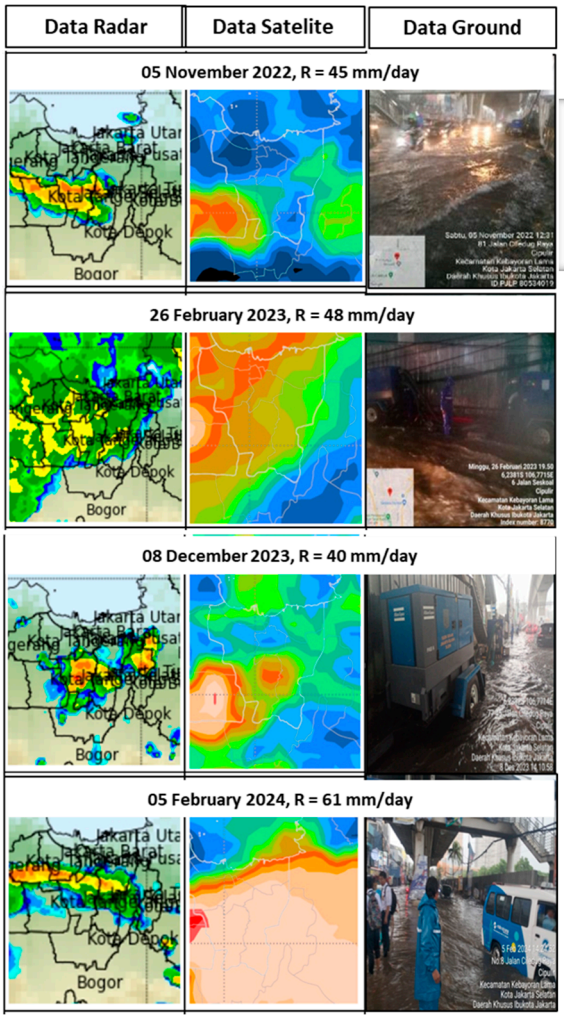


Figure 8. Hourly rainfall distribution pattern of Jakarta Selatan [29].

For high-risk locations, where the flood severity and duration are significant, weather prediction tools play a key role in effective mobile pump deployment. This study compares two weather prediction tools available on the BMKG website: Citra Radar, and Himawari Satellite Imagery. The left-side box in Figure 9 displays a weather radar image, while the right-side box presents satellite-based data.

According to the BMKG, radar images provide real-time depictions of rainfall intensity potential, measured using weather radar reflectivity values. The reflectivity product, expressed in decibels (dBZ), quantifies the amount of radar energy reflected back by water droplets in clouds. Higher dBZ values indicate greater reflectivity, which correlates with stronger precipitation intensity. The maximum effective range of the BMKG's reflectivity product is approximately 240 km from the radar station, with dBZ values ranging from 5 to 75. The color gradient legend ranges from light blue (low intensity) to purple (high intensity), where purple represents the most intense rainfall.

The second weather prediction tool available on the BMKG's platform is the Himawari-9 Satellite Imagery, which detects cloud-top temperatures based on thermal radiation measurements at a 10.4-micrometer wavelength. The imagery uses color coding, where blue and black indicate minimal cloud formation, whereas red and orange signify significant cloud growth, suggesting potential cumulonimbus cloud development.




```
rfe = fs.RFE(model)
rfe = rfe.fit(X_train, y_train)
print('Support', rfe.support_)
print('Ranking', rfe.ranking_)
```

```
Support [ True False]
Ranking [1 2]
```

```
C:\Users\Horas Yosua\AppData\Local\Programs\
was passed when a 1d array was expected. Ple
  y = column_or_1d(y, warn=True)
C:\Users\Horas Yosua\AppData\Local\Programs\
was passed when a 1d array was expected. Ple
  y = column_or_1d(y, warn=True)
```

```
[27]: df1.corr()
```

[27]:

	Radar	Satelite	Cuaca
Radar	1.000000	0.159299	0.760069
Satelite	0.159299	1.000000	0.105467
Cuaca	0.760069	0.105467	1.000000

Figure 9. Radar and satellite imagery of BMKG logistic regression analysis featuring RFE.

A comparative analysis of these two weather prediction tools was conducted based on statistical accuracy, with the findings indicating that BMKG radar reflectivity provides more reliable rainfall detection. As a result, this study recommends BMKG radar as the primary tool for rainfall prediction and mobile pump deployment.

A model-based laboratory test was conducted at the Bandung Institute of Technology (ITB) in 2024 to determine the flood depth threshold associated with floating hazards. The study concluded that a flood depth of 75 cm presents a significant floating risk. From the correlation between rainfall intensity (R) and flood depth (D), it was found that when D reaches 75 cm, R is approximately 138.6 mm/day, corresponding to a return period of 2–5 years. This suggests that a 75 cm flood depth has a 20–50% probability of occurrence.

This study focuses on two primary flood impact factors: flood depth and flood duration. Previous findings indicate that a flood depth of 75 cm or greater occurs at rainfall intensities of 138 mm/day with a 20–50% probability, which is considered to be a high likelihood of occurrence. Since greater flood depths increase the likelihood of prolonged flood durations, this analysis also considers flood duration as a critical factor. The findings suggest that flood durations exceeding 30 min are more common and pose a greater risk than depth alone. Thus, mobile pumps are essential for flood control, and weather prediction tools play a crucial role in preemptive deployment.

To determine the most relevant predictive parameter among three sources (radar, satellite, and BMKG), we carried out a logistic regression analysis (Figure 9) featuring RFE (recursive feature elimination) on a Jupyter Notebook 7.4.0 (release in 2024). This is

a browser-based interface to a Python 3.11 (release in 2024) interpreter. The method is a feature selection technique that is commonly used in machine learning to identify the most significant variables for predictive models. The RFE process ranks features based on their influence on the model's equation. According to the results, the BMKG radar was ranked first, while the satellite data were ranked second.

Additionally, a correlation analysis was conducted to examine the relationship between each variable and weather conditions, where 1 represents rainfall and 0 represents no rainfall. The results, as shown in the corresponding figure, indicate that the radar–weather correlation was 0.760069, significantly higher than the satellite–weather correlation of 0.105467. Based on these findings, this study selected BMKG radar as the primary weather prediction tool.

3.4. Site Selection and HEC-RAS Simulation for Mobile Pump Deployment

According to our analysis of the mobile pump's pressure head using the energy conservation scheme, the increase in pump head can be influenced by several factors:

1. Elevation differences between the mobile pump inlet and outlet: In urban areas, variations in channel elevations are generally minimal.
2. Friction losses in the mobile pump hose: These depend on hose roughness, length, and diameter.
3. Hydraulic resistance caused by bends, contractions, and expansions in the hose: These factors contribute to additional head loss.

As the pump head loss increased, we observed reduced pump capacity, lower pump efficiency, and higher power consumption, as pump efficiency and power demand are inversely related. Thus, increasing the hose roughness, length, bends, or connections will require greater pump power.

Table 3 presents the results of mobile pump deployment optimization, structured as a hierarchical selection process based on hydrological and hydraulic analysis. The hierarchical selection followed the conditions presented in Figure 2. From the initial site selection process (Table 1), ten locations were identified based on flood event frequency in 2022 and 2023. Although none of these sites experienced flood depths exceeding 75 cm, some had flood durations exceeding 30 min, making them eligible for further analysis based on additional criteria, such as mobile pump accessibility and inlet–outlet conditions.

At locations with road widths below 3 m (e.g., Balai Rakyat and Betta), mobile pump deployment was not feasible due to space constraints. This narrowed the selection to eight locations, where mobile pumps could be effectively installed. Among these, four sites had insufficient drainage capacity, while the remaining four required mobile pumps to enhance their water conveyance efficiency.

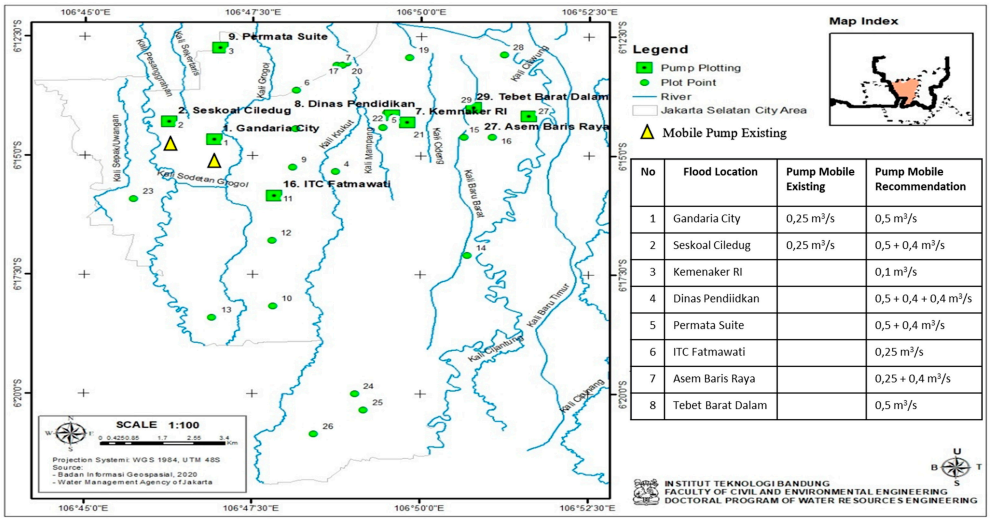
In some areas, more than one mobile pump was needed due to capacity limitations. Additionally, certain locations had inefficient inlet and outlet structures, requiring additional mobile pumps to compensate for the increased head loss. For instance, at the Seskoal Ciledug site, the drainage channel makes two 90-degree turns, resulting in additional head requirements for effective water removal.

After optimizing the placement of mobile pumps across the 29 pluvial flood locations (Figure 10), a detailed hydraulic simulation was conducted for one selected site—Seskoal Ciledug—using HEC-RAS modeling with a mobile pump capacity of 0.5 m^3/s.

Table 3. Site selection for mobile pump deployment optimization.

No Lokasi	Qr 15 mm/h (m^3/d)	Qc (m^3/d)	Qc-Qr 15 mm/h (m^3/d)	Flood Frequency 2022/2023		Impact Flood Depth and Flood Duration	Pump Mobile Access + Inlet Outlet	Radar	Pump Mobile SOP	Mobile Pump Needs (m^3/d)	Placement of Number of Pump Mobile	Number of Pump Mobile	Pump Mobile Stock (m^3/d)
	(2)	(4)	(4-2)										
1 Gandaria City	2.64	2.4	−0.23	8		FD	Y	Y		0.5	13	1	0.1
2 Seskoal Ciledug	0.83	4.82	3.98		16	FD	Y	Y	Y	0.5 + 0.4	14 + 5	2	0.1
3 Mabes Polri	0.67	7.75	7.08		0							3	0.25
4 Terogong Raya	0.85	0.3	−0.55	0								4	0.25
5 Karang Tengah	2.13	1.48	−0.65	0								5	0.4
6 Balai Kartini	2.83	1.23	−1.6	0								6	0.4
7 Kemnaker RI	0.73	3.43	2.69		3	FD	Y	Y		0.1	2	7	0.4
8 Dinas Pendidikan	2.83	0.62	−2.21	5		FD	Y	Y		0.5 + 0.4 + 0.4	10 + 6 + 7	8	0.4
9 Permata Suite	3.12	1.7	−1.41	7		FD	Y	Y		0.5 + 0.4	11 + 8	9	0.4
10 Kemang Raya	0.76	2.33	1.56		0							10	0.5
11 Kapten Tendean	0.67	0.75	0.07		0							11	0.5
12 Jenderal Sudirman	1.98	0.78	−1.2	0								12	0.5
13 Terowongan Jend. Sudirman	1.02	2.58	1.56		0							13	0.5
14 Dharmawangsa Taman Gajah	3.73	13.05	9.32		4	FD				0.1	1	14	0.5
15 RW07 Pondok Labu	0.76	0.15	−0.6	0								TOTAL CAP.	5.2
16 ITC Fatmawati	1.3	2.33	1.02		6	FD	Y	Y	Y	0.25	3		
17 Masjid Al Makmur	0.49	0.15	−0.34	0									
18 FO MT Haryono	0.86	0.33	−0.52	0									
19 Gedung film	1.06	0.33	−0.72	0									
20 Atmajaya	1.02	2.36	1.34		0								
21 Jl. HR Rasuna Said	0.49	0.33	−0.16	0									
22 Semanggi Bawah	1.02	1.44	0.42		0								
23 Komplek Depsos	0.27	0.15	−0.12	0									
24 Balai Rakyat	3.16	0.19	−2.96	2		FD	N						
25 Cupang	0.58	0.03	−0.54	2		FD	N						
26 Batu Belah	3.12	0.08	−3.04	0									
27 Asem Baris Raya	1.08	3.67	2.59		6	FD	Y	Y	Y	0.25 + 0.4	4 + 9		
28 Double Track	3.37	1.02	−2.35	0									
29 Tebet Barat Dalam	2.05	0.33	−1.71	2		FD	Y	N		0.5	12		

In the sixth column of Table 3 there is a column "Impact Flood Depth and Flood Duration". Impact Flood Depth is the height of a potentially dangerous flood with a flood height of more than 75 cm. Impact Flood Depth is abbreviated to (IFD) in the column below if the location has a flood height of more than 75 cm. Meanwhile, Flood Duration is the duration of a flood event that occurs in a flood location. Flood Duration is abbreviated to (FD). If a location has a flood duration of more than half an hour, then the column will be filled with FD. In the table there are FD as many as 11 FD means there are 11 locations that have a flood time of more than 30 min (half an hour).



No	Flood Location	Pump Mobile Existing	Pump Mobile Recommendation
1	Gandaria City	0,25 m^3/s	0,5 m^3/s
2	Seskoal Ciledug	0,25 m^3/s	0,5 + 0,4 m^3/s
3	Kemenaker RI		0,1 m^3/s
4	Dinas Pendiidkan		0,5 + 0,4 + 0,4 m^3/s
5	Permata Suite		0,5 + 0,4 m^3/s
6	ITC Fatmawati		0,25 m^3/s
7	Asem Baris Raya		0,25 + 0,4 m^3/s
8	Tebet Barat Dalam		0,5 m^3/s

Figure 10. Mobile pumps' deployment locations.

The simulation analyzed mobile pump placement configurations using channel cross-sections (Figure 11). The assumed scenario considers that the mobile pump's inlet and outlet are not located within the same channel system, to align with prior manual calculations in the Methodology section. This assumption ensures that outgoing discharge is not influenced by the drainage capacity of the original channel. The simulation results indicate that upstream mobile pump deployment provided the most optimal flood mitigation outcomes (Figure 12). The HEC-RAS calculations in Table 4 confirm that upstream pump placement effectively reduces flood peaks at an early stage. The primary challenge in optimizing this configuration is identifying an alternative channel network to redirect excess water, given the land constraints in urban areas.

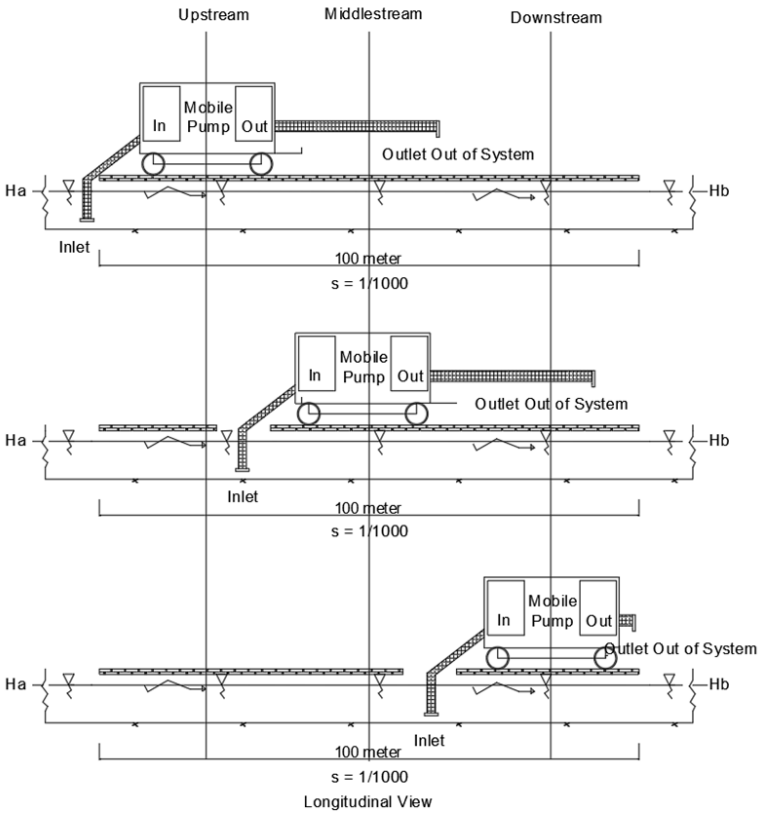


Figure 11. Elongated mobile pump placement configuration.

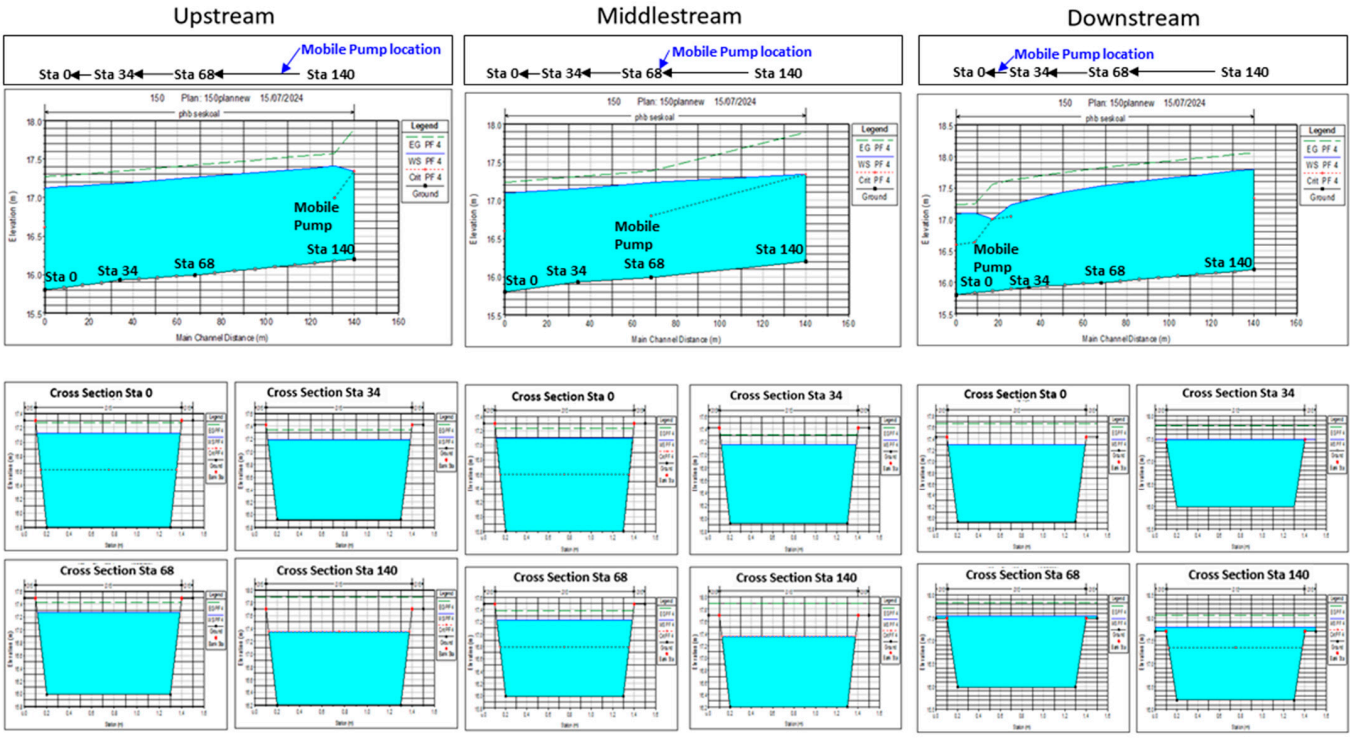


Figure 12. HEC-RAS configuration of mobile pump placement at the Seskoal Ciledug location.

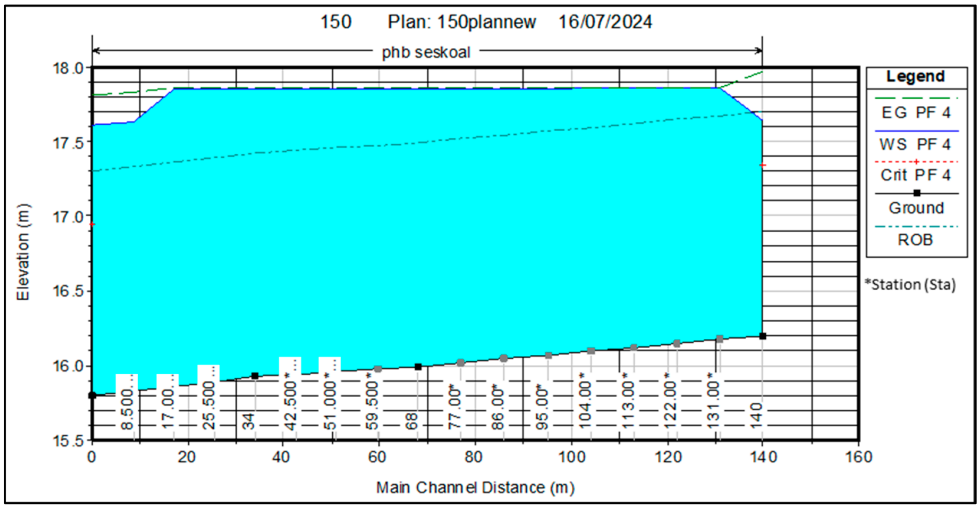
Table 4. Configuration scenarios for various stations and outlets.

Nu	Condition	STA 0	STA 68	STA 140
1	Flood PF discharge 4.4 m^3/d in cm	32	27	22
2	Pump at STA 17 (downstream) out of system in cm	0	5	10
3	Pump at STA 25 (downstream) out of system in cm	0	0	10
4	Pump at STA 25 (downstream) outlet 17 m STA 8 in cm	20	30	30
5	Pump at STA 68 (middle stream) out of system in cm	0	0	0
6	Pump at STA 68 (middle stream) outlet 30 m in cm	30	25	50
7	Pump at STA 131 (upstream) out of system in cm	0	0	0
8	Pump at STA 131 (upstream) outlet 30 m in cm	32	27	22

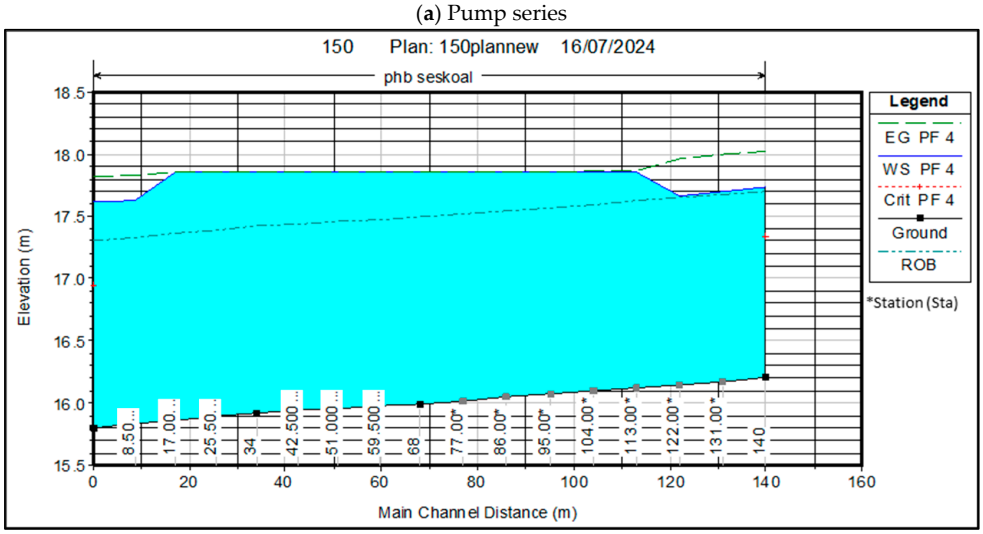
This study also examined single vs. multiple pump configurations, comparing series and parallel installations. The findings reveal that mobile pumps with a parallel setup are more effective than series installations, as they increase discharge capacity. Series mobile pump configurations do not enhance the overall discharge capacity, as additional pumps do not affect the flow rate. We also noticed that deploying two pumps in parallel upstream significantly improved the flood reduction compared to a single pump unit (Figure 13).

In addition to placement optimization, the number of mobile pumps required for each location was assessed (Figure 14). The occurrence of flooding was determined by the difference between inflow and outflow discharge. For instance, in one scenario in which the inflow–outflow discharge difference was 0.33 m^3/s and the flood was 50 cm deep, we noticed that the minimum required mobile pump capacity was 0.3 m^3/s (1 pump unit). Alternatively, two pumps of 0.15 m^3/s each could achieve the same discharge capacity. Since the availability of mobile pumps is limited, this study optimized deployment by selecting pumps with lower individual capacities while maintaining overall efficiency. The simulation results indicate that using one mobile pump (0.15 m^3/s) reduces the flood depth by 30 cm but requires 20 min of operation (from the 28th to the 48th minute). A mobile pump with a larger capacity (0.3 m^3/s) achieves the same result in 10 min (from the 33rd to

the 43rd minute). After usage, these pumps can be relocated to other flood-prone locations, increasing their operational efficiency. Thus, this study's optimization strategy considers both the number and discharge capacity of mobile pumps, ensuring efficient resource allocation for flood mitigation.



(**a**) Pump series



(**b**) Pump parallel

Figure 13. (**a**) Series and (**b**) parallel mobile pump series at the Seskoal Ciledug location.

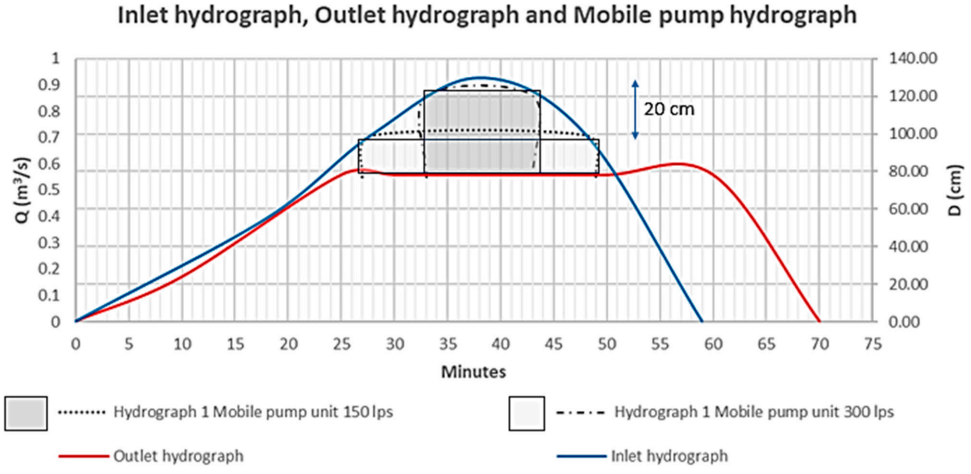


Figure 14. Mobile pump number optimization graph.

To enhance the mobile pumps' performance, we noted that supplementary equipment was required, including mobile pump fittings, a Standard Operating Procedure (SOP) for mobile pumps, and a weather prediction tool (BMKG radar) integrated with the SCADA system. The SOP outlines step-by-step procedures for managing mobile pumps, addressing key operational challenges such as the following:

1. Pre-deployment checks: Ensuring that the pumps are in working condition, free from debris, and ready for deployment.
2. Deployment timing: Activating pumps based on real-time weather data (e.g., from BMKG radar) and flood forecasts to preemptively manage flood risks.
3. Operational monitoring: Continuously assessing pump performance, including inlet and outlet conditions, to maintain optimal functionality.
4. Post-operation maintenance: Cleaning and storing pumps after use to ensure that they are ready for future flood events.

The SOP is integrated into our broader optimization framework for flood mitigation:

- Integration with weather prediction tools: Real-time rainfall data from BMKG radar are used to trigger pump activation at the right time and location, ensuring proactive flood management.
- SCADA system coordination: The SOP works alongside SCADA systems to automate pump operations, enabling remote monitoring and control for efficient deployment.
- Location-specific protocols: At high-risk locations like Seskoal Ciledug, the SOP includes tailored procedures for managing debris accumulation and ensuring clear inlet/outlet conditions.
- Performance metrics: The SOP ensures that mobile pumps maintain flood depths below 75 cm and durations under 30 min, as defined in our risk assessment criteria.

The necessity for an SOP arises from the operational complexities of mobile pumps in urban environments. For instance, among the eight selected locations, only one site does not require radar integration—Inner West Tebet—as it is a dead-end road with no significant traffic disruptions due to flooding. Meanwhile, at locations like Seskoal Ciledug, ITC Fatmawati, and Asembaris, high levels of debris can obstruct pump inlets, leading to reduced efficiency or failure. The SOP addresses these challenges by providing clear guidelines for debris removal, maintenance, and monitoring.

4. Conclusions

Pluvial flooding is an unnoticed problem that exists in urban areas, with different characteristics from fluvial floods, namely, the depth of the flood, the duration of the flood, its complexity, and the availability of land for water channel infrastructure. Solving the pluvial flood problem first requires a study of the channel's ability to receive the planned flood discharge. Flood characteristics, through the correlation of A, D, and R, can be used to determine the cause of existing flood problems. The hourly rain distribution pattern in South Jakarta was in the first two hours, with a percentage weight of 56.6% in the 1st hour and 43.4% in the 2nd hour The mobile pump equipment is a weather prediction tool provided by the BMKG. In this research, radar imagery had the best accuracy. Optimization of mobile pumps and their equipment can be achieved through a hierarchy of sufficient and insufficient channel capacity, flood frequency, high impact and time of flooding, mobile pump entry access, mobile pump SOPs, and equipment. The key achievements of this study are as follows:

- Identification of eight priority locations in South Jakarta for mobile pump deployment, determined through a hierarchical selection process based on channel capacity, flood risk, and accessibility.

- Validation of upstream pump placement and parallel configurations as the most effective strategies for reducing flood depths and durations, supported by HEC-RAS simulations.
- Demonstration of the practical value of integrating real-time weather prediction tools (BMKG radar) with hydraulic modeling for urban flood management.

The optimization framework developed in this study integrates real-time weather data and hydraulic simulations to enhance mobile pump deployment. This approach is adaptable to other urban areas facing similar flood challenges, offering a scalable model for improving flood resilience in densely populated cities by considering factors such as channel capacity, flood risk criteria, and accessibility.

Author Contributions: Conceptualization, H.Y. and M.S.B.K.; methodology, H.Y.; software, H.Y.; validation, H.Y., J.N., E.O.N. and D.S.; formal analysis, H.Y., M.S.B.K., J.N. and E.O.N.; investigation, H.Y.; resources, H.Y.; writing—original draft preparation, H.Y.; writing—review and editing, M.S.B.K., J.N. and E.O.N.; visualization, J.N. and E.O.N.; supervision, M.S.B.K., J.N. and E.O.N.; project administration, H.Y. All authors have read and agreed to the published version of the manuscript.

Funding: This research received no external funding.

Data Availability Statement: The raw data and code supporting the conclusions of this article will be made available by the authors upon request.

Acknowledgments: The authors would like to thank the Water Resources Agency of Jakarta for the data collection required for this article. Furthermore, the authors would also like to express their gratitude to the Water Resources Engineering Research Group of the Faculty of Civil and Environmental Engineering, Institut Teknologi Bandung, for supporting this publication.

Conflicts of Interest: The authors declare no conflicts of interest.

References

1. Guo, K.; Guan, M.; Yu, D. Urban Surface Water Flood Modelling—A Comprehensive review of current models and future challenges. *Hydrol. Earth Syst. Sci.* **2021**, *25*, 2843–2860.
2. Patra, J.P.; Kumar, R.; Mani, P. Combined Fluvial and Pluvial Flood Inundation Modelling for a Project Site. *Procedia Technol.* **2016**, *24*, 93–100. [CrossRef]
3. Tanaka, T.; Kiyohara, K.; Tachikawa, Y. Comparison of fluvial and pluvial flood risk curves in urban cities 582. *J. Hydrol.* **2020**, *584*, 124706. [CrossRef]
4. Yosua, H.; Kusuma, M.B.; Nugroho, J. An assessment of pluvial hazard in South Jakarta based on land use/cover change from 2016 to 2022. *Front. Built Environ.* **2023**, *9*, 1345894. [CrossRef]
5. Edwin, S.S.; Navarun, V.; Zachary, A.S. Evaluation of the normalisasi policy in Jakarta, Indonesia using system dynamics. *Landsc. Arch. Front.* **2019**, *7*, 78. [CrossRef]
6. Kesuma, T.N.A.; Kusuma, M.S.B.; Farid, M.; Kuntoro, A.A.; Rahayu, H.P. An assessment of flood hazards due to the breach of the manggarai flood gate. *Int. J. Geomate* **2022**, *23*, 104–111. [CrossRef]
7. Pratiwi, V.; Yakti, B.P.; Widyanto, B.E. Flood Control Reduction Analysis using HEC-RAS due to Local Floods in Central Jakarta. *IOP Conf. Ser. Mater. Sci. Eng.* **2020**, *879*, 12167. [CrossRef]
8. Sari, V.F.M.; Sutjiningsih, D.; Anggraheni, E. Effectiveness of muara angke polder system in north Jakarta. *Int. J. Innov. Technol. Explor. Eng.* **2019**, *8*, 43–47.
9. Pratama, M.I.; Rohmat, F.I.W.; Farid, M.; Adityawan, M.B.; Kuntoro, A.A.; Moe, I.R. Flood hydrograph simulation to estimate peak discharge in Ciliwung river basin. *IOP Conf. Ser. Earth Environ. Sci.* **2021**, *708*, 012028.
10. Cheng, L.; Lin, H.B.; Zhang, Y.L. Optimization design and analysis of mobile pump truck frame using response surface methodology. *PLoS ONE* **2023**, *18*, e0290348. [CrossRef]
11. Li, S.P.; Lin, H.B.; Zhang, Y.L.; Cheng, L. Static Analysis of Mobile Pump Truck Frame for Four Typical Working Conditions. *Appl. Sci.* **2023**, *13*, 7275. [CrossRef]
12. Kapsiz, M. The efficiency of mobile hydraulic system with diesel engine and axial piston pump analysis. *J. Eng. Res.* **2022**, *10*, 216–228. [CrossRef]

13. Mudhina, M.; Winaya, I.N.A.P.; Parwita, I.G.L.M.; Andayani, K.W. Performance Analysis of Flood Control Buildings Mati River Watershed Area. *Int. Res. J. Eng. IT Sci. Res.* **2023**, *9*, 157–172. [CrossRef]
14. Salim, M.A.; Siswanto, A.B.; Mindiastiwi, T. Study of flood impact handling in Pekalongan District. *IOP Conf. Ser. Earth Environ. Sci.* **2022**, *955*, 012014. [CrossRef]
15. Wu, Y.; She, D.; Xia, J.; Song, J.; Xiao, T.; Zhou, Y. The quantitative assessment of impact of pumping capacity and LID on urban flood susceptibility based on machine learning. *J. Hydrol.* **2023**, *617*, 129116. [CrossRef]
16. Machajski, J.; Kostecki, S. Hydrological analysis of a dyke pumping station for the purpose of improving its functioning conditions. *Water* **2018**, *10*, 737. [CrossRef]
17. Lian, J.J.; Xu, K.; Ma, C. Joint impact of rainfall and tidal level on flood risk in a coastal city with a complex river network: A case study of Fuzhou City, China. *Hydrol. Earth Syst. Sci.* **2013**, *17*, 679–689. [CrossRef]
18. Yosua, H.; Kusuma, M.S.B.; Nugroho, J. Study of flood mitigation system for improving the resilience of pluvial flood control of south Jakarta. (Case study: Ciledug raya, Cipulir.). *IOP Conf. Ser. Earth Environ. Sci.* **2023**, *1169*, 012036. [CrossRef]
19. Nakakita, E.; Sato, H.; Nishiwaki, R.; Yamabe, H.; Yamaguchi, K. Early Detection of Baby-Rain-Cell Aloft in a Severe Storm and Risk Projection for Urban Flash Flood. *Adv. Meteorol.* **2017**, *2017*, 5962356. [CrossRef]
20. Kim, Y.; Hong, S. Very short-term prediction of weather radar-based rainfall distribution and intensity over the Korean peninsula using convolutional long short-term memory network. *Asia Pac. J. Atmos Sci.* **2022**, *58*, 489–506. [CrossRef]
21. Siswanto, S.; van Oldenborgh, G.J.; van der Schrier, G.; Jilderda, R.; van den Hurk, B. Temperature, extreme precipitation, and diurnal rainfall changes in the urbanized Jakarta city during the past 130 years. *Int. J. Climatol.* **2016**, *36*, 3207–3225. [CrossRef]
22. Mori, S.; Hamada, J.I.; Hattori, M.; Wu, P.M.; Katsumata, M.; Endo, N.; Ichiyanagi, K.; Hashiguchi, H.; Arbain, A.A.; Sulistyowati, R.; et al. Meridional march of diurnal rainfall over Jakarta, Indonesia, observed with a C-band Doppler radar: An overview of the HARIMAU2010 campaign. *Prog. Earth Planet. Sci.* **2018**, *5*, 47. [CrossRef]
23. Lestari, S.; Protat, A.; Louf, V.; King, A.; Vincent, C.; Mori, S. Subdaily rain-rate properties in western Java analyzed using C-band Doppler radar. *J. Appl. Meteorol. Climatol.* **2022**, *61*, 1199–1219. [CrossRef]
24. Kumar, P.; Yogeswari, K. Smart Water Management Using SCADA at Water Treatment Plant. *Int. J. Innov. Res. Sci. Eng. Technol.* **2020**, *7*, 5369.
25. Khan, T.A.; Alam, M.; Kadir, K.; Shahid, Z.; Mazliham, M.S. A comparison review based on classifiers and regression models for the investigation of flash floods. *Int. J. Adv. Comput. Sci. Appl. (IJACSA)* **2019**, *10*, 352–359. [CrossRef]
26. Karthik, M.V.; Rahaman, S.A. Flash Flood Warning System Using Scada Systems. *Int. J. Mag. Eng. Technol. Manag. Res.* **2015**, *2*, 68.
27. Fawad, M.; Cassalho, F.; Ren, J.; Chen, L.; Yan, T. State-of-the-Art Statistical Approaches for Estimating Flood Events. *Entropy* **2022**, *24*, 898. [CrossRef]
28. Di Baldassarre, G.; Laio, F.; Montanari, A. Design flood estimation using model selection criteria. *Phys. Chem. Earth Parts A/B/C* **2008**, *34*, 606–611. [CrossRef]
29. Brotowiryatmo, S.H. Review of Rainfall Hourly Distributionon the Island of Java. *J. Civ. Eng. Forum* **2016**, *2*, 145. [CrossRef]
30. Tiyas, N.; Sutjiningsih, D. The influence of land use change and spatial discretization of middle—Lower Ciliwung sub-watershed on flood hydrograph at Manggarai Weir: A preliminary study. *Int. J. Eng. Technol.* **2018**, *7*, 497. [CrossRef]

Disclaimer/Publisher's Note: The statements, opinions and data contained in all publications are solely those of the individual author(s) and contributor(s) and not of MDPI and/or the editor(s). MDPI and/or the editor(s) disclaim responsibility for any injury to people or property resulting from any ideas, methods, instructions or products referred to in the content.